VOL. 21, NO. 10, MAY 2026 ISSN 1819-6608
ARPN Journal of Engineering and Applied Sciences
©2006-2026 Asian Research Publishing Network (ARPN). All rights reserved.
www.arpnjournals.com

MACHINE LEARNING-ASSISTED RECONFIGURABLE DUAL-BAND WEARABLE PATCH ANTENNA FOR BODY-CENTRIC IoT APPLICATIONS

P. Santosh, Bondla. Maha Lakshmi, R. Umamaheswari, T. Sri Deepika, Y. M. S. R. Krishna, K. Yeswanth and Shaik Ansar Bibi
Department of Electronics and Communication Engineering, Vignan's Institute of Information Technology (A), Visakhapatnam, India
E-Mail: santoshpavada@vignaniit.edu.in

ABSTRACT

Due to fluctuating wireless settings and signal strength degradation caused by human body impacts, reconfigurable antennas using machine learning methods are seeing more applications in body-centric Internet of Things devices. For the purpose of reconfiguring frequency bands, this study presents the construction of a miniature wearable dual-band patch antenna with a PIN diode. Antennas of this kind work well in the 2.44 GHz and 5.09 GHz ranges. By using signal metrics like RSSI and SNR, an adaptive switching circuit is designed using a machine learning approach. This model is then utilised to identify the optimal frequency range. We can see that the gain is within 7 dBi, the specific absorption rates are within safety limits, and the impedance matching is within an acceptable range (S11 > -15 dB) from the simulation results. The developed wearable antenna can withstand bending conditions, making it ideal for use in wearable applications.

Keywords: wearable antenna, machine learning, reconfigurable antenna, body-centric IoT, dual-band antenna, adaptive communication.

Manuscript Received 9 April 2026; Revised 5 May 2026; Published 20 July 2026

1. INTRODUCTION

Extensive research has been conducted on flexible wearable antennas with the aim of improving the dependability of body-centric communication [1]. In terms of construction, materials, and applications, a thorough evaluation of wearable antennas was provided in [8] and [7]. Radiation loss and surface area ratio (SAR) were among the topics covered by the writers while discussing wearable antennas. Having said that, the majority of the antennas shown here were not adaptable. In [2], [19], and [22], the authors examined the effectiveness of wearable antennas for body-centric communication. The writers emphasized the need of wearing antennas being small, flexible, and safe. Having said that, the antennas discussed in this article couldn't be changed [18]. In [3] and [4], the topic of wearable antennas in the context of next-generation communication technologies was discussed. Improving the performance and bandwidth of wearable antennas was the main emphasis of the writers. There was no way to change the configuration of the antennas described in this piece. In their work on wearable antennas for ISM and 5G, the authors introduced dual-band and wideband designs in references [4][21][26][28]. There was no way to change the configuration of the antennas described in this piece.

Wearable antennas with reconfigurability enabled by PIN diodes have been detailed in [5][6][8][25]. The authors introduced intelligently designed wearable antennas that can switch frequencies. Optimisation of antenna designs using machine learning was introduced by the authors in [9]. A reconfigurable wearable antenna with increased bandwidth was introduced by the authors in [10][13]. Wearable antennas made of textiles and powered by PIN diodes were introduced in [11] [15]. For use in WLAN and ISM networks, the authors of [12] [14] [16] [22] developed a small, flexible antenna with two bands.

The aforementioned research shows that the majority of current wearable antenna designs use either narrow frequency bands or reconfigurability techniques. Reconfigurable wearable antennas that use PIN diodes can operate on several bands, but they can't adapt to changing conditions since they don't have any intelligence. The use of machine learning approaches in reconfigurable band selection for wearable IoT devices is still in its early stages, despite its use in antenna design and optimization. Therefore, a smart and adaptable antenna system that can choose the best frequency band on the fly in reaction to changing signal circumstances is required.

For Internet of Things (IoT) applications focused on the human body, this study proposes a smart reconfigurable dual-band wearable patch antenna that makes use of machine learning. To provide reconfigurability between two distinct operating bands, the suggested antenna makes use of a PIN diode. The optimal communication band is chosen based on signal metrics such as the Received Signal Strength Indicator (RSSI) and the Signal-to-Noise Ratio (SNR). A smart system that uses machine learning to do this is also presented. A microcontroller unit controls the PIN diode's biasing circuit, which allows the intelligent system to make a choice. This will enable adaptive communication using the suggested antenna, which is well-suited for real-time applications because of its ability to adjust its working bands in response to the ever-changing wireless environment.

©2006-2026 Asian Research Publishing Network (ARPN). All rights reserved.

2. ANTENNA DESIGN AND GEOMETRY

A tiny, versatile, dual-band patch antenna is recommended for use in body-centric Internet of Things applications. The antenna's built-on-a-foam substrate takes advantage of the material's lightweight construction and low dielectric constant to maximize radiation efficiency while minimizing electromagnetic losses. An antenna's structural elements include a substrate, a ground plane, and a rectangular microstrip patch. On the top surface of the substrate is placed the micro strip patch, and on the bottom surface is placed the ground plane. Antenna feeding and impedance matching are both performed via the micro strip line.

The standard micro strip antenna design equations were used to calculate the dimensions of the rectangular pattern. The width of the patches is found by

$$\boldsymbol{W}=\frac{c}{2f_r}\sqrt{\frac{2}{\varepsilon_r+1}} \quad (1)$$

In the equation, g denotes the speed of light, f is the resonant frequency, and ε is the substrate dielectric constant. The patch effective length is estimated as follows.

$$\boldsymbol{L}=\frac{c}{2f_r\sqrt{\varepsilon_{eff}}} \quad (2)$$

Where ε_{eff} is the effective dielectric constant of the substrate.

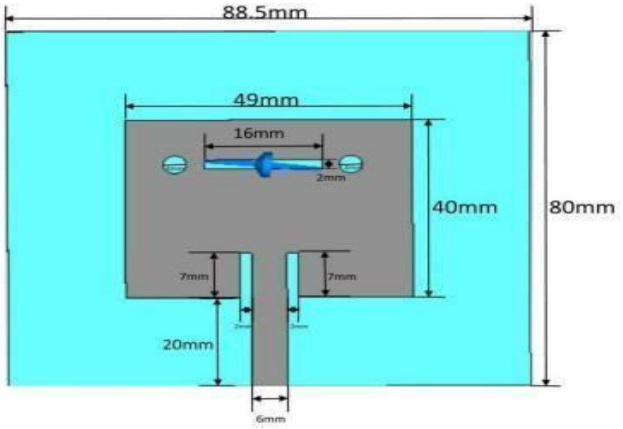


Figure-1. Geometry of the Reconfigurable Patch antenna showing the PIN-Diode Slot Bridge.

The radiation pattern is modified by inserting a rectangular slot in such a manner that the current distribution is altered, resulting in the acquisition of numerous resonant frequencies. The ability to reconfigure the frequency is achieved by connecting a PIN diode over the slot bridge. By preventing current from flowing through the slot when turned ON, the PIN diode operates at a single frequency range. By simulating an open circuit when turned off, the PIN diode may generate a second resonant band. This is how a reconfigurable antenna for the Internet of Things focused on the body is created.

3. MACHINELEARNINGBASEDPIN-DIODESWITCHING

The PIN diode is utilized for frequency reconfiguration in the proposed antenna system by modifying its switching state. The PIN diode is often biased externally by a circuit that controls the switching of the device. An antenna's electrical path is altered by the biasing circuit. To enhance the switching process, this system suggests using a machine learning approach. The biasing circuit and the machine learning model are connected by a microcontroller.

Received Signal Strength Indicator (RSSI) and Signal-to-Noise Ratio (SNR) are two wireless signal metrics that the suggested system takes into account while feeding data into the machine learning model. The machine learning model uses these factors to determine the optimal communication frequency range. The suggested model chooses a different band if the current band's signal strength is poor or if interference is detected. The microprocessor predicts the state of the PIN diode and then regulates it by sending the necessary control signals to the bias circuit. By selecting Band-1, the antenna is able to function at a lower frequency band without the diode being turned on. Selecting Band-2 causes the diode to turn on, enabling the antenna to function in the higher frequency band.

©2006-2026 Asian Research Publishing Network (ARPN). All rights reserved.

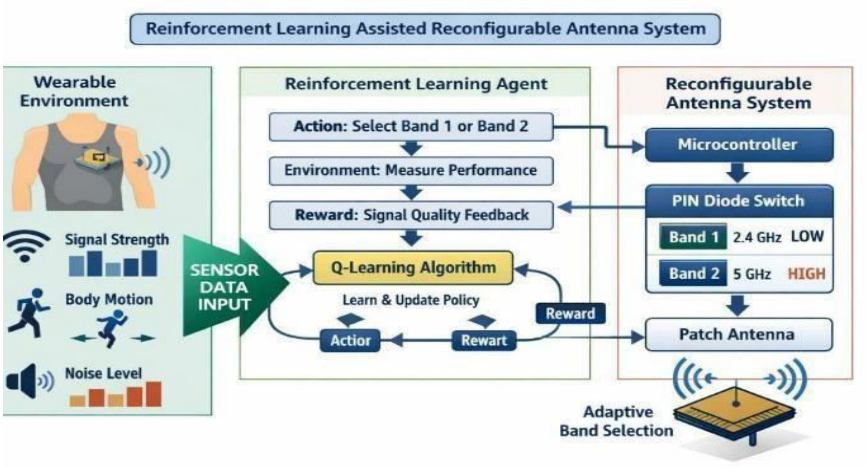


Figure-2. Block diagram of a reconfigurable antenna system for adaptive band selection assisted by machine learning.

3.1 Sample Data Set

The optimal operating band is determined by the machine learning model's analysis of signal properties like RSSI and SNR. Table I shows a simple illustration of the rationale used to pick bands.

Table-1. Example Decision Logic for Band Selection.

RSSI (dBm)	SNR(dB)	Selected Band	PIN diode state
-85	8	Band-1	OFF
-75	12	Band-1	OFF
-65	18	Band-2	ON
-60	20	Band-2	ON

4. PARAMETRIC ANALYSIS AND PERFORMANCE EVOLUTION

Indication of the proposed antenna was not done in a single attempt. Rather, it developed over time through several phases of refining, in which every change was presented on the basis of the observations made on the previous. It was this process which helped us to know how individual geometrical and electrical modifications had an effect on the behavior of the antenna. The following development is explained in subsections.

4.1 Stage-1: Initial Patch Response

A basic inset-fed rectangular patch was used to build the antenna, which resonates in the 2.45 GHz ISM band and is based on the conventional micro strip theory. There were no tuning features or changeable parts at this stage; instead, the focus was on making sure the estimated dimensions, feed structure, and substrate material were accurate for the experiment. Subsequent modifications, such as inset modifications, slot integration, and diode switching, were tested against this baseline to determine their impact on electrical behavior.

Figure-3 shows the simulated S_{11} response for this first setup, with resonances at around 2.45 GHz and 4.0 GHz.

©2006-2026 Asian Research Publishing Network (ARPN). All rights reserved.

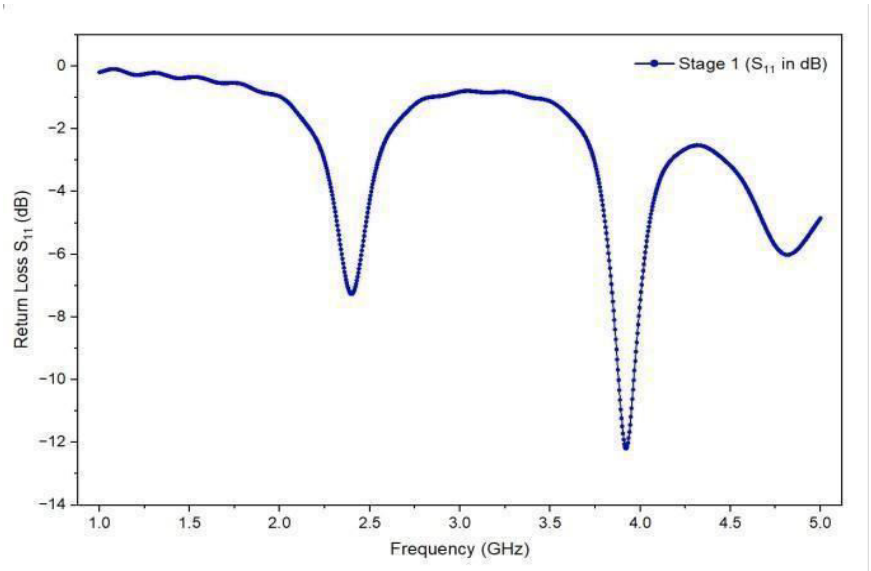


Figure-3. Initial Patch Response Plot (S_{11}).

4.2 Stage2 Vs Stage3: Feed Optimization and Slot-Loaded Response

In order to equalize the impedance and permit the usage of alternative resonance modes, the antenna was adjusted with the inset-feed depth after the Initial Patch Response was set up in Stage 1. One important way to reduce return loss is to tilt the insert position so that the load on the gearbox line is in line with the currents on the patch surface. Iterative optimization helped choose a 10 mm inset feed length as the most economical, which allowed for a noticeable improvement in the multi-band's behavior. Stage 2's more highly notched and resonance-filled simulated response (blue curve in Figure-3) highlights the significance of feed refinement in improving coupling and matching efficiency.

A rectangle and two circular slots were carved into the patch in Stage 3 to enhance spectral control and stabilize the resonant bands even more. These characteristics allow one to intentionally change existing routes, which in turn allows one to actively stimulate higher-order modes while avoiding undesirable resonances. With improved impedance performance and several resonances reaching values below -15 dB, the revised return-loss curve (red trace in Figure-4) indicates a superior multi-band response. There is a significant improvement in the identification and spacing of resonances compared to Stage 2. This demonstrates that the antenna's mode selectivity and spectrum utility are substantially increased with the incorporation of slot loading, making it more suitable for use in wearable IoT systems that need high-quality, multi-frequency performance.

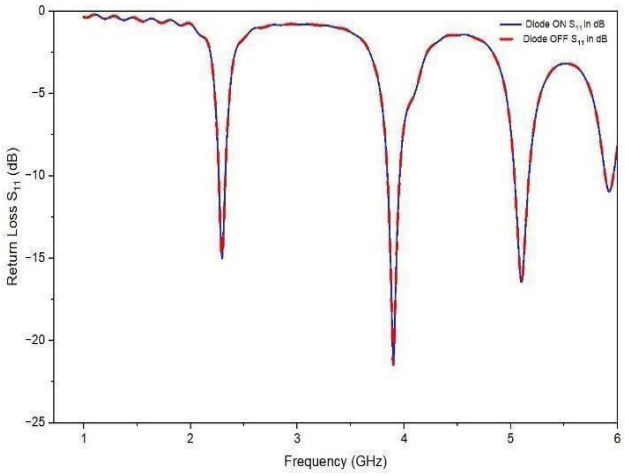


Figure-4. Baseline Patch Antenna Geometry.

4.3 Stage 4 and Stage 5-Reconfigurable Operation Using PIN Diode Switching

The next stage of development, after achieving a stable multi-band response with feed, is tuning and slot integration, which is focused on enabling electrical reconfigurability. In order to do this, a rectangular hole was cut into the analytically insulated BAR64-04PIN diode, allowing the antenna to alter the surface current distribution in response to the diode's state. Essentially, the diode reduces the slot length and changes the resonance behavior when turned on, acting as a low-impedance bridge with values of R = 2.2 Ω, L ≈ 6 nH, and C ≈ 0.02 pF.

The diode's high-impedance discontinuity, on the other hand, resets the original mode and returns the slot length when turned off. Dynamic switching is made possible by this process. Control of mechanical resonances is achieved without requiring any structural modifications. Figure-5 shows the simulated switching states of S-1 compared to one another.

©2006-2026 Asian Research Publishing Network (ARPN). All rights reserved.

While it establishes functional reconfigurability, there seems to be a presence of turn-loss curves, and precise changes in resonant frequencies do occur. That the integration of diodes does not diminish antenna performance is crucial, since the impedance matching is just below the -10 dB threshold of key ISM and WLAN bands. At this stage, there is a distinction to consider. Create a multi-band radiator that is electrically passive. A platform that can be adjusted to meet the communication needs of many wireless services; this allows a single tiny antenna to function. Additionally, the design's suitability for wearables is confirmed by the stability throughout both modes.

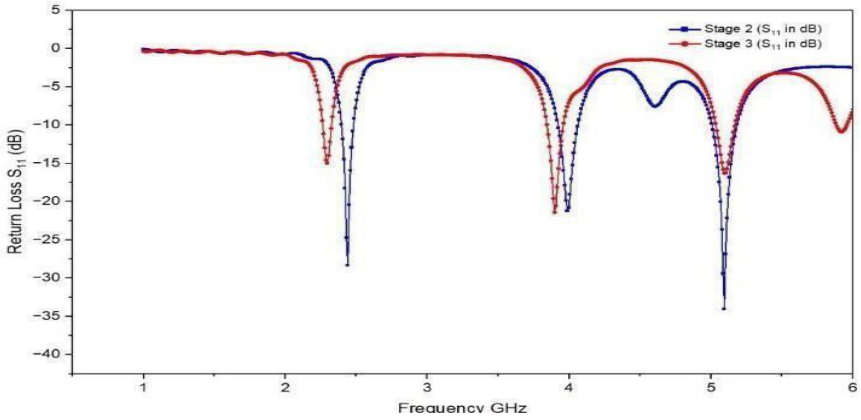


Figure-5. Stage2VsStage3: Feed optimization and slot- loaded response.

4.4 Reinforcement Learning Based Switching Analysis

The Q-learning algorithm's convergence behavior under various signal situations is shown in Figures 6 and 7. Over the course of many episodes, the model is trained by updating the Q-values according to the reward that is earned for each action.

The Q-values rise and level off with the number of events in both the weak signal (State 0) and strong signal (State 1) scenarios. That the reinforcement learning model has learned the best course of action for every situation is evident. Although some initial oscillations may be attributed to exploration, the model is able to attain a stable policy for adaptive band selection, as confirmed by the convergence of the curves.

This proves that the suggested switching mechanism aided by machine learning is effective.

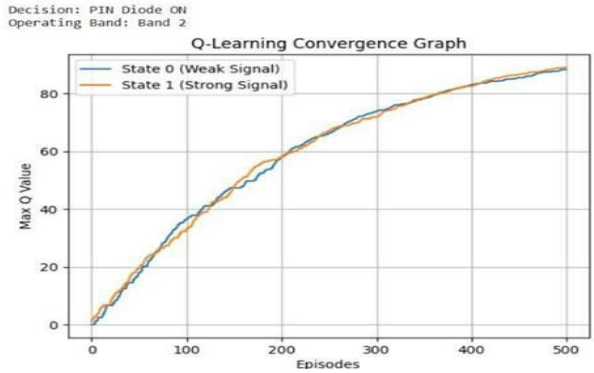


Figure-6. Q-learning convergence graph when the diode is on.

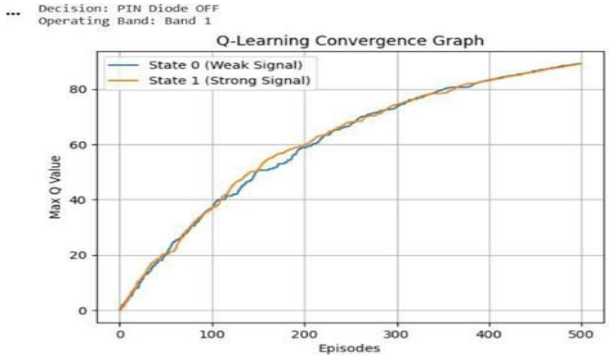


Figure-7. Q-learning convergence graph when the diode is off.

4.5 Surface Current Distribution

The proposed antenna can be frequency agile by reconfiguring it through a PIN diode, and the density of current was measured as the resonant frequencies, which are predominant in the return loss characteristics, are shown in Figures 8 and 9, to validate the switching mechanism.

Figures 8 and 9 show the current graphs for the appropriate ON and OFF switches. When turned on, the diode is in the PIN state (Figure-8). Functions as an electrical short circuit, linking the slot and forming a continuous current flow inside the radiating structure. A high and consistent current concentration is tracked along the feed line, the central slot area, and the top patch border. The electrical length can be increased with the help of this continuity. Specifically, the radio's resonances at lower frequencies, about 4.1 GHz and 6.43 GHz, must be maintained. Confirmation of the significant current concentration at the slot edges is also provided. According

©2006-2026 Asian Research Publishing Network (ARPN). All rights reserved.

to the notion of multi-band reconfigurable antennas mentioned in the literature, different resonant modes may be feasible due to the inductive nature of the diode's switching.

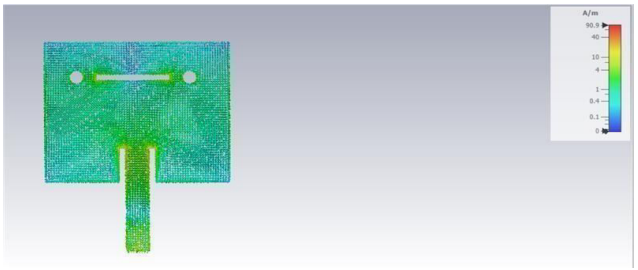


Figure-8. Surface Current Distribution (Diode ON Condition).

In contrast, when the PIN diode is turned off (Figure-8). The present route is discontinuous with respect to the slot, given that the diode exhibits open-circuit behavior. Consequently, most of the current flows through the feed, reducing the active electrical length, the transition area, and the lower radiator portion. A current distribution is all that is available. Represents the same as the observed increase. Oscillations, which are equivalent to the maximum value of the S11 in its off state. The fact that there isn't much buzz about the position confirms its validity. The antenna enters a smaller electrical mode with lower reactive storage, as seen by capacitive behavior when turned off. From a comparative analysis, the PIN diode does more than just turn on and off. It actively participates in electromagnetic transformations. It provides a route of conduction, allowing for selective tuning of resonance. Thus avoiding the deterioration of radiation stability. Another piece of evidence is the fact that the currents at a given location are neither distorted nor asymmetrical.

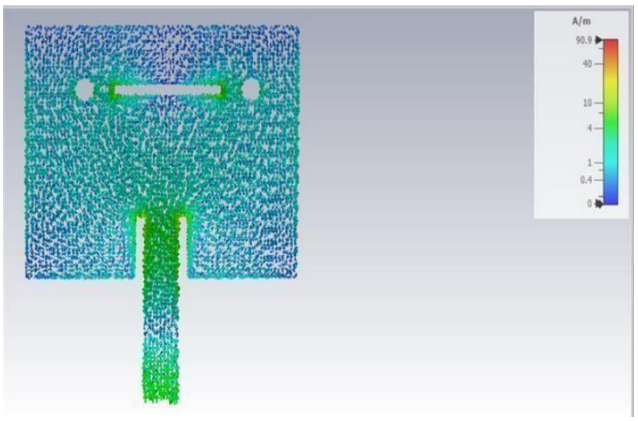


Figure-9. Surface Current Distribution (Diode OFF Condition).

4.6 Radiation Performance and Realized Gain Evaluation

The radiation characteristics of the proposed antenna were evaluated across the operational bands to validate its suitability for wearable and IoT-based operation. The assessment includes realized gain performance under normal and diode-switched conditions, bending influence, and far-field radiation pattern behavior at representative resonant frequencies.

A. Radiation Pattern Analysis

The radiation properties of the proposed antenna are analyzed by the H-plane and E-plane radiation patterns for the operating frequencies of 2.44 GHz and 5.09 GHz for both switching states. The results show that the proposed antenna has stable and consistent radiation properties.

The antenna has a nearly unidirectional radiation pattern in the H-plane and a stable directional pattern in the E-plane at a frequency of 2.44 GHz, when the PIN diode is OFF. This shows effective radiation, making it suitable for body-centric communication systems.

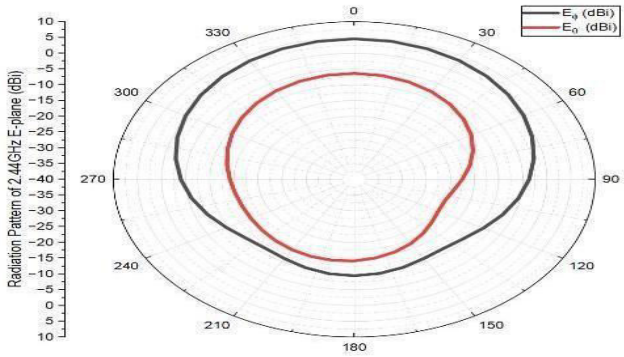


Figure-10. E-plane radiation pattern of the proposed antenna at 2.44GHz.

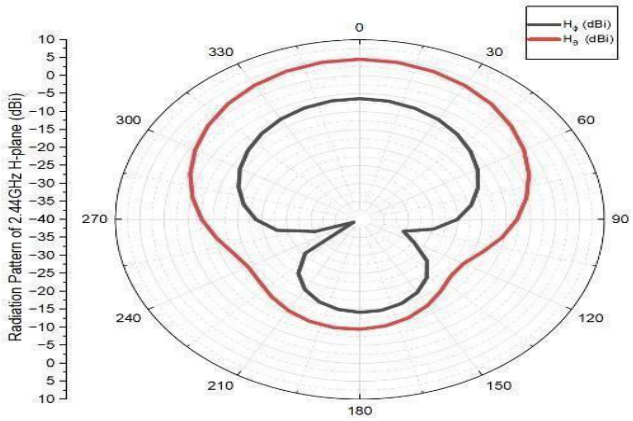


Figure-11. H-plane radiation pattern of the proposed antenna at 2.44 GHz.

The radiation patterns remain constant at 5.09 GHz, with modest shape fluctuations induced by the switching mechanism's shift in current distribution. Reliable functioning at higher frequencies is confirmed by the antenna's strong directivity and lack of substantial distortion or nulls.

©2006-2026 Asian Research Publishing Network (ARPN). All rights reserved.

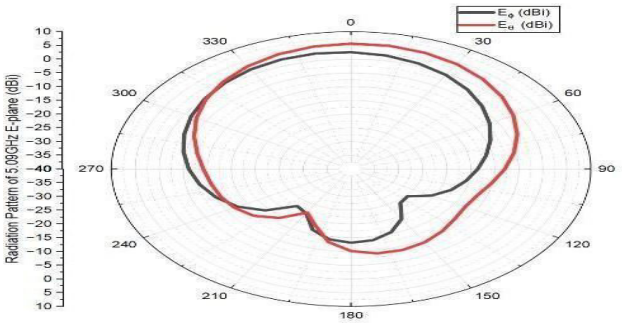


Figure-12. E-plane radiation pattern of the proposed antenna at 5.09GHz.

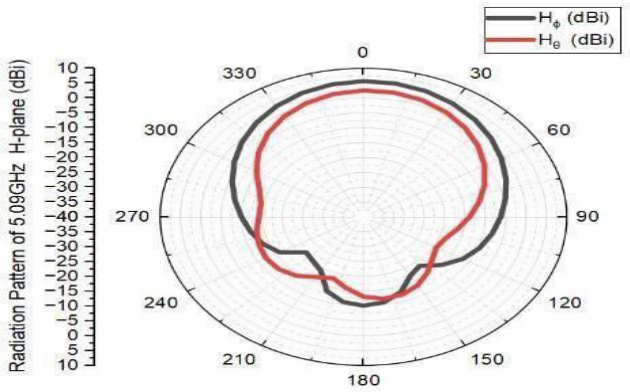


Figure-13. H-plane radiation pattern of the proposed antenna at 5.09 GHz.

Thus, the radiation patterns for both planes and operating bands show that the proposed antenna's radiation properties are consistent with frequency reconfiguration. The success of the antenna's design relies heavily on the PIN diode's switching mechanism.

B. Realized Gain Evaluation under Normal and Reconfigurable Mode

The gain that was achieved for both PIN-diode states throughout the frequency sweep is shown in Figure-10. The gain profile stays consistent in both ON and OFF circumstances, displaying a range of roughly 1.3 dBi to 6.6 dBi, depending on the operating frequency. The structure shows a deeper impedance mismatch before slot stabilisation in earlier phases, with the lowest reported at 3 GHz and the maximum near 7 GHz.

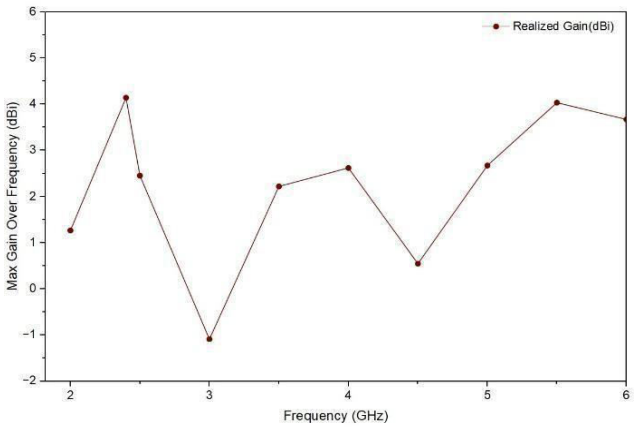


Figure-14. Realized Gain Evaluation Under Normal and Reconfigurable Mode.

The almost simultaneous traces of ON/OFF gain demonstrate that the diode state influences frequency tuning without degrading the radiation strength of the antenna-a crucial characteristic for quick, wearable applications where reconfigurability should not sacrifice radiation strength. This conclusion is in agreement with earlier findings in wearable reconfigurable systems, where it is expected that semiconductor switching would result in negligible radiation losses when adequately insulated on flexible boundaries.

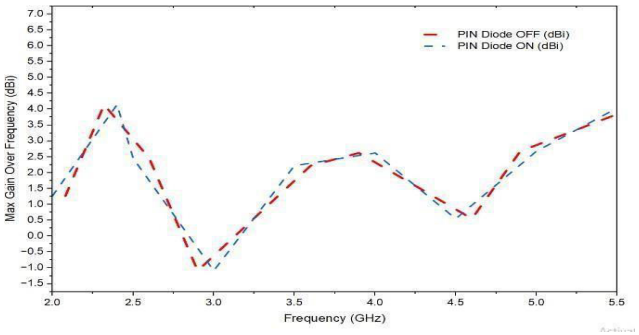


Figure-15. Realized Gain Evaluation under Normal and Reconfigurable Mode of pin-diode.

4.7 Bending and Wearability Evaluation

A. Bending Influence on Gain Stability

It is expected that the wearable antenna would be placed on the curved surface of the human body; therefore, the radiation characteristics of the proposed antenna under bending conditions are also presented. Figure-11 illustrates the realized gain of the proposed antenna under bending conditions against frequency. It is clear that the antenna has a stable gain performance over a frequency range of 2 to 8 GHz with slight changes from −1.1 dBi to 6.6 dBi. These changes at specific frequencies are mainly due to changes in the surface current distribution of the antenna while it is placed on the curved surface of the body. Nevertheless, it has been observed that no significant degradation in radiation performance has occurred, despite

©2006-2026 Asian Research Publishing Network (ARPN). All rights reserved.

these differences. This proves that the antenna can withstand stress without breaking. Additionally, the antenna exhibits effective radiation properties even when it is bent, as there are no deep nulls or severe oscillations. This is mostly because detuning is lessened by the flexible foam substrate and the grounded-backed antenna arrangement. This proves that the suggested antenna is viable for wearable devices and will function appropriately whether put on various areas of the human body, such as the arm, chest, or torso. The suggested antenna may be used on non-planar human surfaces, such as the arm or chest, in IoT networks, thanks to the use of the flexible foam substrate and the ground-backed arrangement, which allows for steady gain.

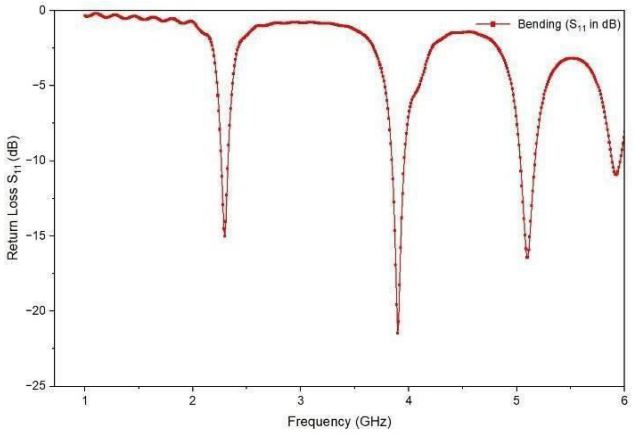


Figure-16. S11 response under bend.

In order for the suggested antenna to be employed in wearable and body-centric Internet of Things applications, its electromagnetic properties must be preserved under deformation situations. There are a number of real-world reasons why a wearable antenna might bend in an application. These include the user's motion or the antenna being attached to a non-planar surface, such as an arm, chest, or torso. Consequently, a bending analysis is carried out in this work.

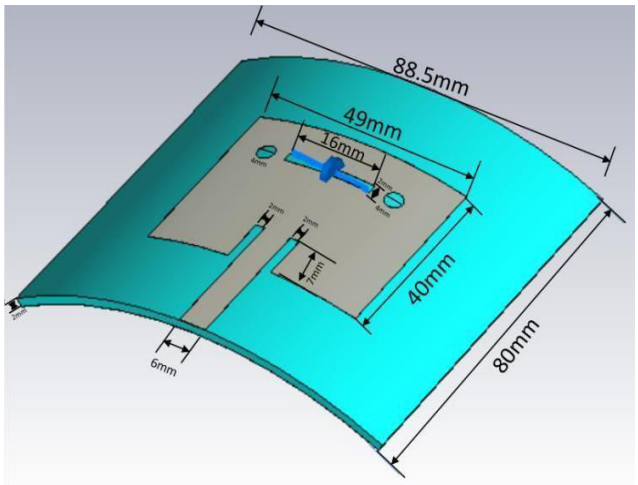


Figure-17. Final bending antenna.

There was an analysis of the realized gain trend under bent operation to further quantify the impact of bending on radiation performance. Across all working bands, there are only small variations to the gain fluctuation, which are well within acceptable limits. This phenomenon is typical of mechanically flexible antennas and is mainly explained by the redistribution of light current and changes in effective electrical length induced by substrate curvature.

That the flexible substrate, ground-backed design, and slot-based tuning all work together to reduce detuning effects is confirmed by the observation of nose recovery and the deterioration of sudden resonance loss. In most cases, the bending test verifies that the antenna in question maintains stable electromagnetic functioning even when subjected to substantial deformation, meaning that it is mechanically durable and operates reliably. The antenna's ability to maintain a continuous wireless connection in dynamic on-body applications is shown by its consistent S11 response and conserved gain behavior. This makes it a good fit for body-centric IoT and wearable sensors.

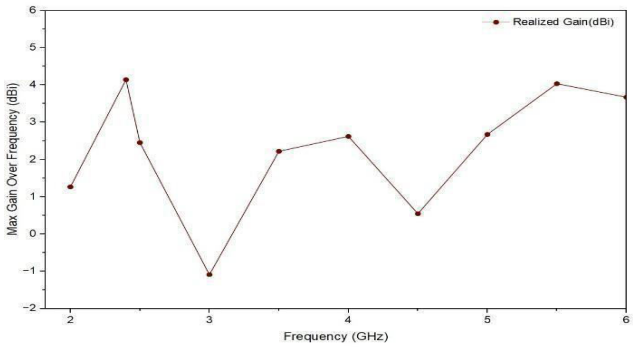


Figure-18. The realized gain plot under bent operation.

4.8 SAR Analysis

As the proposed antenna is for continuous wearable application, the electromagnetic exposure limit needs to be satisfied. For this purpose, the Specific Absorption Rate (SAR) analysis was performed for the proposed antenna. The antenna was placed in direct contact with the phantom without any gap, as the direct contact between the antenna and the phantom is a worst-case scenario for wearable IoT devices such as medical monitoring straps and textile-based wearable communication devices.

The simulated peak SAR values were evaluated for both reconfigurable states of the antenna. The maximum SAR value was found tobe0.987W/kg when the PIN diode was in the OFF state, and it was found to be 1.085 W/kg when the diode was in the ON state. These values are much lower than the FCC limit of 1.6 W/kg, which should be averaged over 1g of tissue, and are much lower than the ICNIRP and IEEE C95.1 limit of 2.0 W/kg, which should be averaged over 10g of tissue. The small difference between the two states shows that the reconfiguration mechanism has little effect on the

©2006-2026 Asian Research Publishing Network (ARPN). All rights reserved.

antenna's interaction with human tissue, confirming the safety of the antenna for both states.

5. RESULTS AND DISCUSSIONS

A comparative summary of representative wearable and reconfigurable antenna designs is presented in Table-2. Existing flexible wearable antennas, such as [R1], provide good body-centric performance but lack frequency reconfiguration, limiting their adaptability to dynamic IoT environments. Similarly, foam- and textile-based antennas [R2], [R3] offer low SAR and stable bending performance, but operate in fixed frequency bands without switching capability. Although PIN- diode-based reconfigurable antennas [R4], [R5] provide frequency agility, they are often rigid or semi-flexible and do not incorporate intelligent adaptation mechanisms.

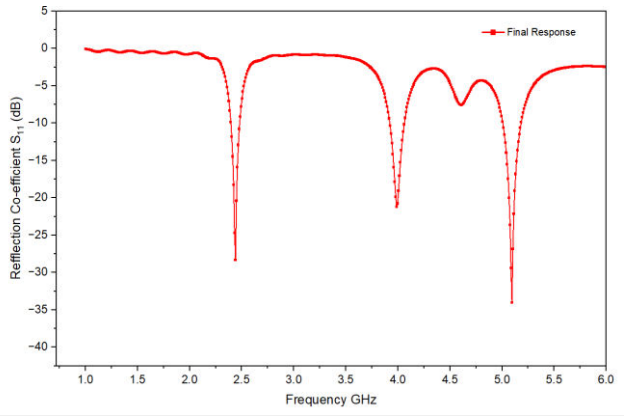


Figure-19. Final antenna results.

Table-2. Performance summary of the proposed antenna.

Parameter	Diode OFF (Band-1)	Diode ON(Band-2)
Operating Frequency(GHz)	2.44 GHz	5.09 GHz
Return Loss(dB)	-28.32 dB	-34.05dB
VSWR	1.6	1.6
Peak Gain(dBi)	6.6 dBi	6.6 dBi
Gain Range(dBi)	1.3 - 6.6 dBi	1.3 - 6.6 dBi
Bandwidth(MHz)	200MHz	300MHz
SAR(W/Kg)	0.987W/kg	1.085W/kg
Radiation Stability	Stable	Stable
Bending Effect	Minimal variation	Minimal variation
ML Adaptation	Active	Active

The suggested antenna gets beyond these restrictions by integrating a machine learning-assisted switching mechanism with PIN-diode-based reconfigurability. While operating on a flexible foam substrate, the antenna functions in dual frequency bands (2.44 GHz and 5.09 GHz), exhibiting steady performance even when bent. It also maintains low SAR values. By including a reinforcement learning (Q-learning) model, the ideal operating band may be dynamically selected using real-time signal metrics like RSSI and SNR, which is not possible with traditional designs. Efficient band selection under varied wireless settings is guaranteed by the reinforcement learning findings, which show convergence and steady decision-making. It is evident from the findings that the suggested reconfigurable wearable antenna can operate in dual-band with frequencies of 2.44 GHz and 5.09 GHz, having excellent impedance matching with S11 <−15 dB bandVSWR< 2. Moreover, even when bent, the antenna maintains continuous radiation characteristics and has steady gain values of up to 6.7 dBi. In addition, the suggested antenna is suitable for wearable applications since the computed SAR values of 0.987 W/kg under OFF circumstances and 1.085 W/kg under ON conditions are much lower than the protective limitations. In addition, the suggested Q-learning method uses the machine learning model to guarantee the communication process's dependability. Table-3 describes the Comparison of the proposed antenna with Representative Wearable/Reconfigurable Design.

©2006-2026 Asian Research Publishing Network (ARPN). All rights reserved.

Table-3. Comparison of proposed antenna with representative wearable/reconfigurable design.

Ref.	Substrate Type / Flexibility	Reconfigurable	Bands (GHz)	SAR / Bending	Peak Gain (dBi)	Findings vs. Proposed Antenna
[R1] Awan *et al.*, 2023	Textile (Flexible)	No	2.45 / 5.2	SAR only	3-5	Lacks reconfigurability; only dual-band, good flexibility
[R2] Pathak *et al.*, 2024	Foam (Flexible)	No	3–10 (UWB)	SAR & Bending	2-4	UWB but fixed band; lacks control over band selection
[R3] Abdelghany *et al.*, 2024	Jeans (Flexible)	No	2.45 / 5.8	SAR	2.15-3.08	Low SAR but no switching or additional bands
[R4] Musa *et al.*, 2023	Rogers 5880	Yes (PIN)	2.4 / 5.8	Limited	~6	Reconfigurable but not fully flexible or wearable-tested
[R5] Palsokar & Ghosh, 2021	FR4 (Rigid)	Yes (PIN)	2.4 / 3.5 / 5.8	No SAR	4-5	Good switching but unsuitable for wearable bending
[R6] Singh *et al.*, 2025	Silicone / PDMS (Flexible)	No	2.4 only	Wearable	~3	Single-band wearable; lacks IoT multi-standard support
[R7] Salvado *et al.*, 2025	Textile	No	2.45 only	SAR	~2-3	Good comfort but outdated and fixed frequency
Proposed Antenna	Foam (Flexible)	Yes (PIN + ML)	2.44 / 5.09	SAR & Bending Stable	Up to 7	Reconfigurable, ML-assisted adaptive band selection

6. CONCLUSIONS

A reconfigurable dual-band wearable patch antenna for body-centric IoT devices is the intended outcome of the proposed study. This antenna may be reconfigured between 2.44 GHz and 5.09 GHz. It is constructed with a foam substrate and features a PIN diode. Critical parameters including VSWR, gain, and reflection coefficient are investigated by computational modelling. With an impedance bandwidth of S11 <-15 dB, VSWR < 2, and a maximum gain of 6.7 dBi, the suggested antenna is considered satisfactory. The suggested antenna can also endure situations when it is bent. Its applicability to wearable technology is confirmed by the fact that its Specific Absorption Rate (SAR) is within acceptable ranges.

In order to further enhance the overall performance of the system, a Q-learning model has also been used, and an adaptive switching mechanism based on machine learning has been included. Intelligent identification of the system's ideal frequency band is achieved in the suggested model by the use of signal metrics like RSSI and SNR. A microprocessor has also been used to automatically regulate the PIN diode's biasing circuit, which has resulted in the expected output. Possible future directions include integrating the suggested system with a variety of wearable IoT devices, implementing the system in real-time hardware, and improving decision-making via the application of sophisticated machine learning methods. As a potential option for smart healthcare applications and body-centric communication systems, the suggested antenna design might potentially be expanded for multi-band and next-generation wireless applications.

REFERENCES

[1] S. Singh, R. Mishra, A. Kapoor and S. Singh. 2025. A comprehensive review and analysis of the design aspects, structure, and applications of flexible wearable antennas. Telecom. 6(1): 3.

[2] A. G. Al-Sehemi *et al*. 2019. Wearable antennas for body-centric communications. ACES Journal, vol. 34, no. 3, pp. 259-270.

[3] S. R. Kale. 2024. A review of wearable antennas for 5G and body-centric wireless communication. PIMI Journal.

©2006-2026 Asian Research Publishing Network (ARPN). All rights reserved.

[4] U. K. Kommuri. 2024. Dual-band and wideband wearable antenna designs for ISM and 5G remote health monitoring. In IGI Global.

[5] A. A. Palsokar *et al*. 2020. Frequency and pattern reconfigurable rectangular patch antenna using PIN diodes. AEÜ - Int. J. Electron. Commun.

[6] Ł. Januszkiewicz *et al*. 2025. Dual-band wearable antenna integrated with glasses for visually impaired support systems. Applied Sciences. 15(14).

[7] H. Yalduz and O. A. Civi. 2020. Design and analysis of low-profile and low-SAR full-textile dual-band wearable antenna for WLAN. AEÜ - Int. J. Electron. Commun.

[8] Y. Thangavelu *et al*. 2024. Design and SAR analysis of an AMC-integrated wearable antenna. Micromachines. 15(12).

[9] U. Musa *et al*. 2025. Machine learning-optimized dual-band wearable antenna for IoT applications. Scientific Reports.

[10] D. Kumar *et al*. 2024. Novel design of a bandwidth-enhanced and frequency-reconfigurable wearable antenna for body-centric communication. J. Electromagn. Eng. Sci.

[11] Q. H. Dang *et al*. 2025. A frequency reconfigurable wearable textile antenna with one PIN diode. Telecommunication and Radio Engineering. Vol. 84.

[12] M. Brenda *et al*. 2025. Design and characterization of compact dual-band flexible antenna for 2.4/5.5 GHz WLAN/ISM applications. AEÜ - Int. J. Electron. Commun.

[13] N. H. Shehab *et al*. 2014. Design of dual-band wearable antenna using metamaterials. in Proc. Int. Conf. Antennas and Propagation.

[14] [14] K. V. Karad *et al*. 2024. SAR analysis of hexagonal-shaped UWB antenna for wearable applications. EURASIP J. Wireless Commun. Netw.

[15] A. O. Elrashidi and A. Shehata. 2024. Flexible dual-band dipole-type wearable antenna for remote health monitoring at 2.4 GHz and 5.2 GHz. IEEE Access. 12: 120598-120608.

[16] R. Singh *et al*. 2024. SAR reduction and bending impact analysis of an EBG-based wearable patch antenna. Int. J. Intelligent Systems and Applications in Engineering. 12: 59-66.

[17] M. Wagih, Y. Wei and E. Li. 2021. Mechanical effects on textile antennas for IoT and body-area networks. IEEE Internet of Things Journal. 8(10): 7989-7999.

[18] P. Raut and S. Deshmukh. 2024. Slot-loaded flexible patch antenna for multiband IoT wearable devices. IETE Journal of Research. 71(6): 832-841.

[19] S. Verma, R. Patel and M. Parida. 2019. L-shaped defective ground wearable antenna for multiband operation. in Proc. IEEE ICAC3. pp. 321-325.

[20] A. Singh and M. K. Mandal. 2017. Compact dual-band reconfigurable antenna using PIN diode switching. IEEE Trans. Antennas Propag. 65(7): 3352-3356.

[21] A. Kiourti and K. S. Nikita. 2012. Recent advances in implantable and on-body antennas. IEEE Antennas and Propagation Magazine. 54(3): 210-228.

[22] M. Kalpana *et al*. 2025. Design and performance analysis of a wheel-shaped microstrip patch antenna for multiband applications. In Proc. IEEE WAMS, Chennai, India.

[23] P. Santosh *et al*. 2025. Pick-and-place robotic vehicle with arm. In Lecture Notes in Electrical Engineering, Springer. pp. 487-496.

[24] P. Santosh *et al*. 2025. A compact wide-band array antenna for Ka-band applications. Journal of Communications. 20(3): 349-357.

[25] S. Velicheti *et al*. 2023. Design of conformal log periodic dipole array antennas using different shapes of top loadings. Progress in Electromagnetics Research M. 116: 91-102.

[26] K. Chitambara Rao *et al*. 2021. Design, simulation and experimental validation of patch antenna in S-band satellite communication. In Lecture Notes in Electrical Engineering, Springer. pp. 477-489.

[27] P. Santosh and P. Mallikarjuna Rao. 2021. Enhancement of bandwidth and VSWR of double notch E-shaped inset-fed patch antenna. In Lecture Notes in Electrical Engineering, Springer. pp. 349-356.

©2006-2026 Asian Research Publishing Network (ARPN). All rights reserved.

[28] D. Prabhakar *et al*. 2020. Design and development of antenna array using slots for multiband applications. Journal of Advanced Research in Dynamical & Control Systems. 12(6).

[29] S. P. Pavada *et al*. 2019. Enhancement of bandwidth using inset-fed patch antenna for high-frequency applications. Int. J. Engineering and Advanced Technology. 9(1): 1528-1531.

[30] D. Kumar and D. Mathur. 2024. Novel design of a bandwidth-enhanced and frequency reconfigurable wearable antenna for body-centric communication. Journal of Electromagnetic Engineering and Science. 24: 2640275.

[31] Konkyana, L. B., Rekha, V. S. D., Kumar, J. P., Santosh, P., Addepalli, T., Kumar, S. V., Medasani, S., Balaji, M., Gamini, S., & Devireddy, S. R. (2026). Design of single element penta band, high directive gain antenna for 5g mm wave applications. Telecommunications and Radio Engineering, 85(5), 63–72.

[32] C. V. Sivaramprasad, P., Santosh et al., "Hierarchical graph attention network with bidirectional LSTM for real-time multi-class network intrusion detection," Journal of Theoretical and Applied Information Technology, vol. 104, no. 12, Jun. 2026.